JTTEE5 17:721–727
DOI: 10.1007/s11666-008-9245-6
1059-9630/$19.00 © ASM International

Microstructure and Mechanical Properties of Low-Pressure Cold-Sprayed (LPCS) Coatings

Heli Koivuluoto, Juha Lagerbom, Mikko Kylmälahti, and Petri Vuoristo

(Submitted May 7, 2008; in revised form September 9, 2008)

In low-pressure cold spraying, compressed air is used as a process gas. The most important process parameters are temperature and pressure. In the Low-Pressure Cold Spraying (LPCS) system in this study, the maximum preheating temperature is 650 °C and pressure is 9 bar. Powders used in LPCS process contain alumina with metallic powders; therefore LPCS is the method to spray soft metallic coatings with ceramic hard phase for different application areas, e.g., thick coatings and coatings for electrical and thermal conduction and corrosion protection applications. The aim of this study was to investigate microstructure, denseness, and mechanical properties of LPCS Cu, Ni, and Zn coatings. LPCS coatings seemed to be dense according to Scanning Electron Microscope (SEM) studies but corrosion tests were needed to identify the existence of porosity. Through-porosity was observed in structures of the LPCS coatings. Bond strengths of LPCS Cu and Zn coatings were found to be 20-30 MPa, and hardness was high indicating reinforcement and work hardening.

Keywords copper, low-pressure cold spraying, mechanical properties, microstructure, nickel, zinc

1. Introduction

Cold spraying was developed in the former Soviet Union in the 1980s. Cold spraying is regarded as the latest development in the thermal spray techniques. The process is based on the utilization of significantly lower process temperatures with high particle velocities than those in other thermal spray methods. A coating is formed when powder particles impact at high velocities (high kinetic energy) on the substrate, deform, and adhere to substrate or to other particles. Moreover, good bonding between the cold-sprayed powder particles needs a high degree of plastic deformation upon the particle impact (Ref 1, 2). In low-pressure cold spraying (LPCS), preheating temperatures of the process gas (air) are between room temperature (RT) and 650 °C, and pressures are between 5 and 9 bar. Typically, compressed air is used in this method as the process gas to spray powder mixtures (Ref 3). Particle velocities are reported to be approximately from 350 to 700 m/s in the low-pressure cold spray process (Ref 4). Irissou et al. (Ref 5) have reported particle velocities of 580 m/s for Al_2O_3 particles (mean size 25.5 μm). In addition, Ning et al. (Ref 6) have updated mean particle velocities of 450 m/s for Cu particles (30 μm) (sprayed with helium). Furthermore, irregular particles have reportedly higher in-flight velocities compared to spherical particles (Ref 6) possibly explaining the utilization of dendritic particles in the some cases (e.g., Cu and Ni) in LPCS process.

Low-Pressure Cold-Sprayed (LPCS) is the method to spray metallic powders (e.g., Cu, Al, Ni, Zn) with an addition of ceramic powder in the blended spray powder. Different substrate materials, e.g., metals, ceramics, and plastics, can be used. The main functions of the ceramic addition are the activation of the sprayed surfaces and the cleaning of the nozzle of the gun. In addition to these, ceramic particles are affected by mechanical hammering of the substrate/sprayed layers or by the so-called shot peening via particle impacts (Ref 7). Ceramic addition in the powder also has a compacting effect during the impact, indicating influences on coating properties and improved deposition efficiency (Ref 8). Shkodkin et al. (Ref 8) have reported increased bond strength and coating density with increasing ceramic addition. The amount of ceramic particles in the sprayed coating is low compared to initial powder composition. Usually, coatings contain ceramic particles below 5% of the total amount of ceramic powder (Ref 8). This indicates the erosion occurrence of and also activation by ceramic particles (Ref 8, 9). A hard phase

This article is an invited paper selected from presentations at the 2008 International Thermal Spray Conference and has been expanded from the original presentation. It is simultaneously published in *Thermal Spray Crossing Borders, Proceedings of the 2008 International Thermal Spray Conference*, Maastricht, The Netherlands, June 2-4, 2008, Basil R. Marple, Margaret M. Hyland, Yuk-Chiu Lau, Chang-Jiu Li, Rogerio S. Lima, and Ghislain Montavon, Ed., ASM International, Materials Park, OH, 2008.

Heli Koivuluoto, Juha Lagerbom, Mikko Kylmälahti, and **Petri Vuoristo**, Department of Materials Science, Tampere University of Technology, P.O. Box 589, 33101 Tampere, Finland. Contact e-mail: heli.koivuluoto@tut.fi.

can be used for the purpose of reinforcement to strengthen the metallic matrix in LPCS process (Ref 10). Low-pressure cold spraying has many advantageous features, e.g., possibility to produce thick coatings, use in repair and shape modification of molds (Ref 3, 8). Low-pressure cold spraying or radial injection gas dynamic spray (RIGDS) reportedly have applications in the fields of aerospace, automotive, and rebuild industries (Ref 2).

Copper has good electrical and thermal conductivity (Ref 11); therefore it has been used often as a well-conducting coating material. Furthermore, nickel has good corrosion-resistance in many corrosion environments (Ref 12). Zinc is also a good corrosion resistant material for applications in which corrosion protection is provided by cathodic protection of steels. Zinc coatings act as a sacrificial anode protection (Ref 13). Zinc coatings are, therefore, mostly used only for corrosion protection, e.g., in car industry (Ref 3).

The aim of this study was to characterize microstructures of LPCS Cu, Ni, and Zn coatings and to get more information about the denseness of these coatings by corrosion studies. Moreover, mechanical properties (hardness and bond strength) on grit-blasted steel and copper substrates were investigated to get more information about coatings, and, as well as the influences of hard, ceramic phase on the coating properties.

2. Experimental Procedure

In this study, LPCS Cu, Ni, and Zn coatings were prepared at Tampere University of Technology with a DYMET 304 K equipment. Compressed air was used as a process gas. Spraying parameters are summarized in Table 1. DYMET equipment was installed into an x-y manipulator. A round (Ø 5 mm) tubular nozzle was used in this study. Substrates were grit-blasted (mesh 24, Al_2O_3 grits) steel and copper plates with the dimensions of 100 × 50 × 5 mm.

Three commercial powders were tested in LPCS process. Figure 1 shows the morphologies of copper powder K-01-01 (Cu + 50vol.-%Al_2O_3), nickel powder K32 (Ni + 50vol.-%Al_2O_3), and zinc powder K-0011 (Zn + 50vol.-%Al_2O_3) from OCPS (Obninsk Center for Powder Spraying). Copper and nickel powders were electrolytically prepared, having a dendritic structure, whereas zinc powder was atomized and possessed a spherical shape. With all these powder mixtures, the ceramic particles in the metal/ceramic powder blends were a fused and crushed alumina (Al_2O_3), having a blocky and irregular shape.

LPCS coatings were characterized using a Philips XL30 Scanning Electron Microscope (SEM). The microstructures of LPCS coatings were studied from metallographic cross sections (unetched and etched structures). LPCS Cu coating was etched with an etching solution of 95 mL ethanol, 5 g $FeCl_3$ and 2 mL HCl. Denseness, and especially through-porosity of the LPCS coatings, was tested with corrosion tests, open-cell electrochemical potential measurements, and salt spray (fog) test. The electrochemical cell used in the open-cell potential measurements consisted of a tube, of diameter 20 mm and volume 12 mL, glued on the surface of the coating specimen. A 3.5 wt.% NaCl solution was poured into the tubes for

Table 1 Spraying parameters of LPCS coatings. Beam distance stands for distance between two adjacent spray beads

Spraying parameter	LPCS Cu	LPCS Ni	LPCS Zn
Pressure, bar	6	6	6
Preheating temperature, °C	540	540	440
Powder feed, g/min	20	15	24
Traverse speed, m/min	6	6	6
Beam distance, mm	1	1	1
Spraying distance, mm	10	10	10
Number of layers	2	7	2

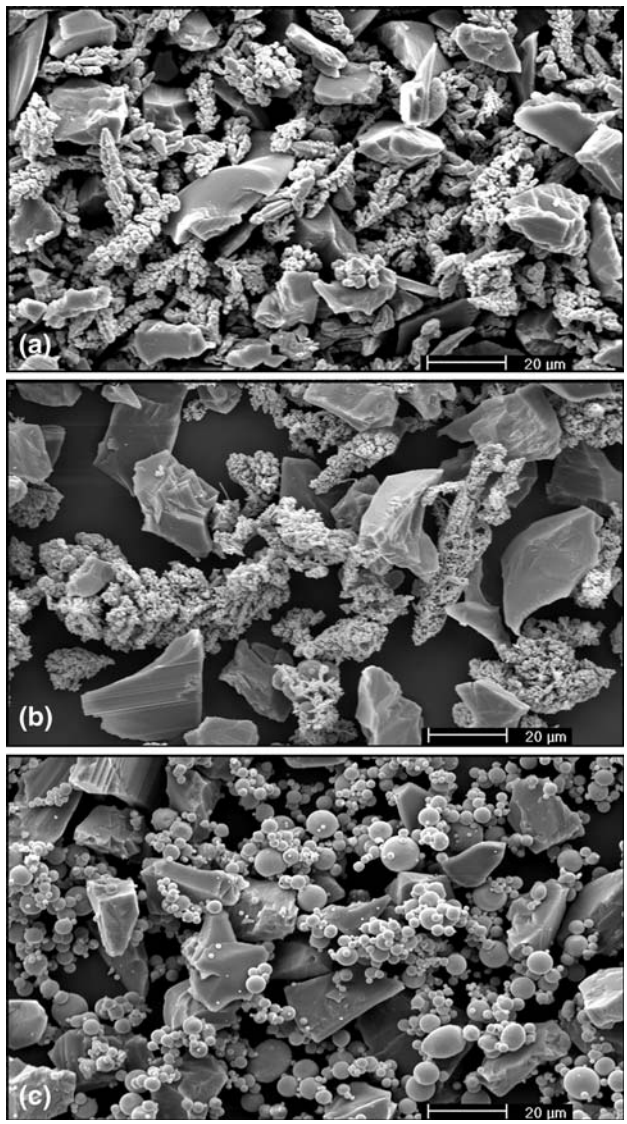

Fig. 1 Morphologies of powders (a) Cu + Al_2O_3, (b) Ni + Al_2O_3, and (c) Zn + Al_2O_3 used in LPCS process

nine-day measurements. Open-cell potential measurements were done with a Fluke 79 III true RMS multimeter. A silver/silver chloride (Ag/AgCl) electrode was used as a reference electrode. Salt spray fog test was done according to the ASTM B117 standard. A 5-wt.% NaCl solution was used with an exposure of 96 h, a temperature of 35-40 °C, a solution pH of 6.3, and a solution accumulation of 0.04 mL/cm^2 h. Samples were visually examined before, during, and after exposure.

Mechanical properties, hardness, and bond strength were also tested. Vickers hardness ($HV_{0.3}$) was measured as an average of ten measurements with a Matsuzawa MMT-X7 hardness tester. Bond strength values were determined according to the standard EN582 in a tensile pull test (Instron 1185 mechanical testing machine). Three measurements were carried out to calculate the average values of bond strength or in this case cohesive strength because of fracture planes (more details later).

3. Results and Discussion

The microstructural details, i.e., microstructure and denseness (existence of through-porosity) were investigated in this study. In addition, mechanical properties, hardness and bond strength, were obtained to gain more information about coating properties.

3.1 Microstructure of LPCS Coatings

Microstructures of LPCS Cu, Ni, and Zn coatings on grit-blasted steel substrates were investigated with SEM (SE and BSE images) analysis (Fig. 2, 3, and 4, respectively). In the microstructures of LPCS Cu, Ni, and Zn coatings, the detected black particles are Al_2O_3, arising from the powder mixture. The thickness of LPCS Cu coating was 200 μm. According to visual examination, LPCS Cu coating seemed to be dense without any noticeable pores (Fig. 2a). However, some oxidized areas (dark gray areas) between particle boundaries are detected in the coating structure (Fig. 2b, BSE image). LPCS Cu coating was etched to reveal the real cross-sectional microstructure. Powder particle boundaries cannot be noticed in the microstructure but the primary particle boundaries can be observed from the etched microstructure (Fig. 2c). It is possible that powder particle with dendritic structure breaks down during the particle impact on the surface of substrate or other particles. Moreover, flattened shape of primary particles indicates that high degree of plastic deformation occurred during spraying.

Figure 3(a) presents the microstructure of LPCS Ni coatings. The thickness of LPCS Ni coating was 290 μm. LPCS Ni coating was relatively dense according to visual observation. However, some open boundaries can be detected near the coating surface and some oxidized boundaries can be observed in the coating structure (Fig. 3b). Oxidation was mostly concentrated in the primary particle boundaries in the structure of LPCS Cu and Ni coatings, which is shown in Fig. 2(b) and 3(b).

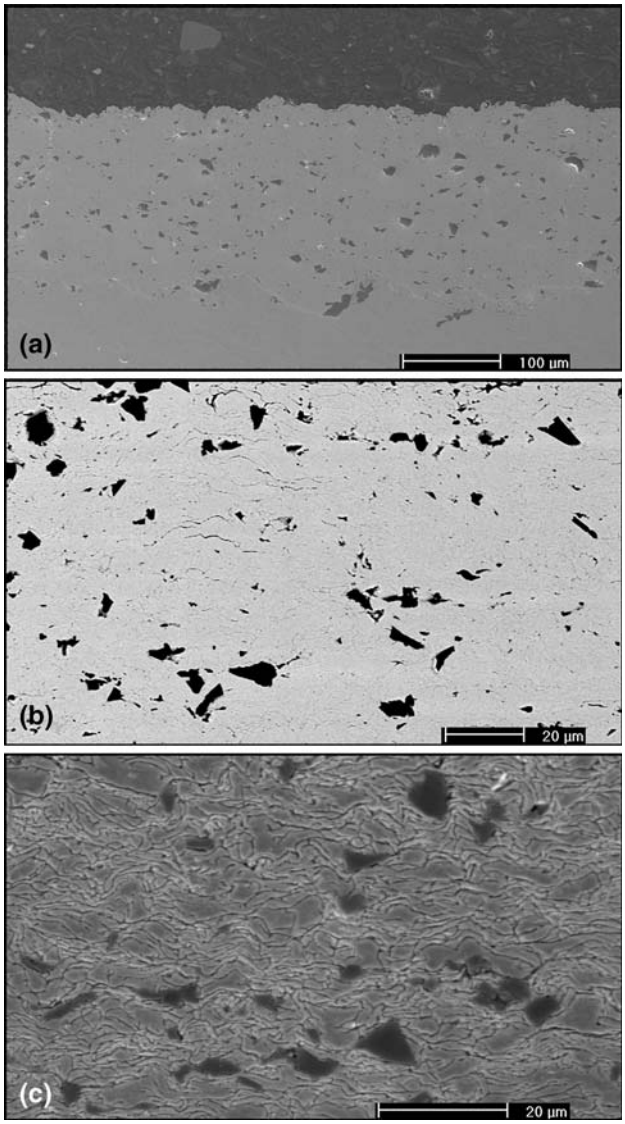

Fig. 2 LPCS Cu coating on grit-blasted steel substrate (a) SE image, (b) BSE image, and (c) SE image, etched microstructure

As-received powder particles had an oxidized layer on the surface caused by the electrolytic production method of the powder. Dendritic particles have large surface areas and, hence, more oxidized areas than on the surface of, e.g., atomized spherical particles. In addition, it is possible that powder particles oxidized during spraying because air was used as a process gas. Thus, oxidized boundaries in the coating structure were possibly originated both from oxidized layers in the powder particles and from oxidation during spraying (both during in-flight and on the substrate).

The detected black particles in the LPCS Zn coating also were Al_2O_3 particles on the gray metallic matrix (Fig. 4). The thickness of LPCS Zn coating was 150 μm. The structure of LPCS Zn coating by BSE image (SEM) differs from the structure of LPCS Cu and Ni coatings because of the different types (shape, production method)

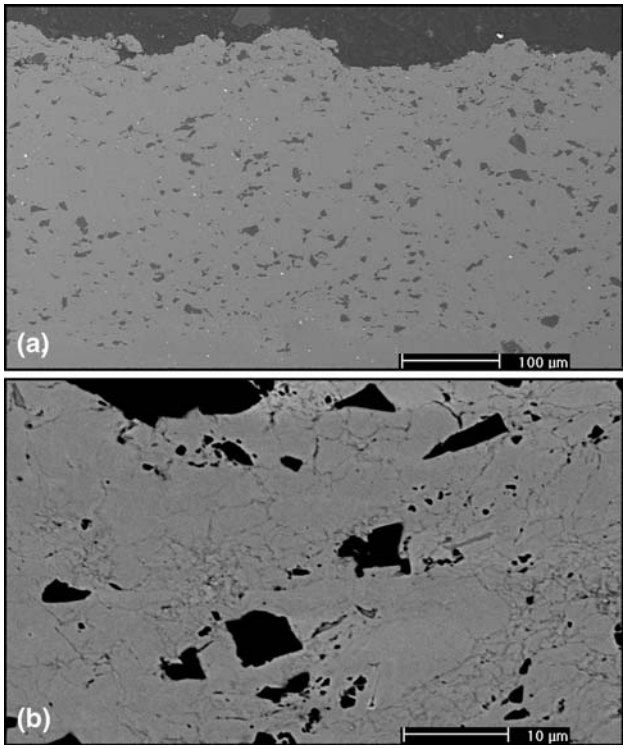

Fig. 3 LPCS Ni coating on grit-blasted steel substrate (a) SE image and (b) BSE image

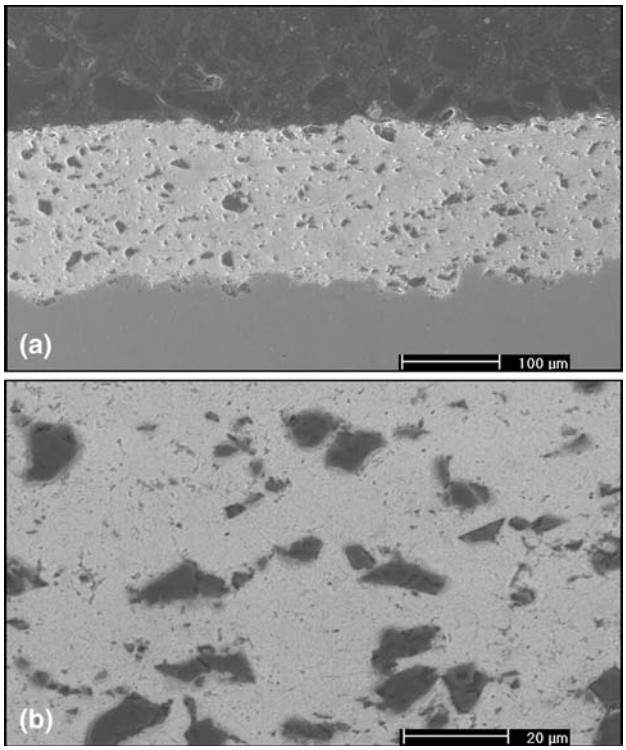

Fig. 4 LPCS Zn coating on grit-blasted steel substrate (a) SE image and (b) BSE image

of powders. Zinc powders were atomized, whereas nickel and copper were electrically prepared. Particle boundaries (initial state spherical particle shape) were imperceptible from unetched structure, indicating visually dense microstructure (Fig. 4b). Besides, it should be noticed that low amount of porosity in zinc coatings can be allowed because the steel substrate is in any case protected cathodically by the zinc coating. In summary, LPCS Cu, Ni, and Zn coatings were dense according to visual evaluation by SEM. Noticeable pores were not observed in the coating structures; nevertheless, some oxidized areas or boundaries can be detected especially in the LPCS Ni coating.

3.2 Denseness of LPCS Coatings

LPCS coatings were found to be quite dense according to SEM examinations. Furthermore, denseness was investigated with corrosion tests to get more information about existing through-porosity (open-porosity). The corrosion tests used were open-cell potential measurement and salt spray fog test.

Open-cell potentials of LPCS Cu and Ni coatings are presented in Fig. 5 and 6 as a function of exposure time. During the exposure, the behavior of the LPCS Cu coating was compared to the behavior of bulk Cu plate and

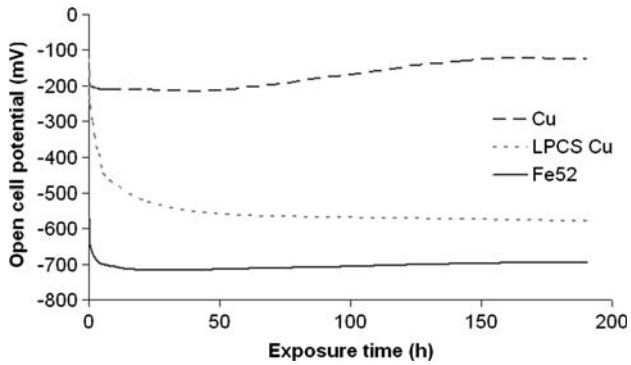

Fig. 5 Open-cell potential of Cu bulk material, LPCS Cu coating, and Fe52 substrate material as a function of exposure time (Ag/AgCl reference electrode)

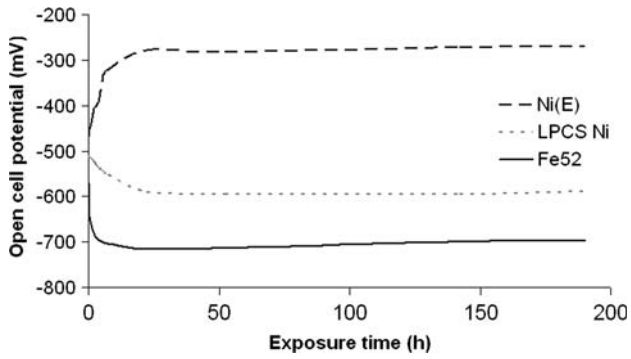

Fig. 6 Open-cell potential of electrolytically prepared Ni coating (Ni(E)), LPCS Ni coating, and Fe52 substrate material as a function of exposure time (Ag/AgCl reference electrode)

substrate material Fe52 plate to find out existing porosity. When open-cell potential curve of the coating is close to the curve of bulk material, it indicates denseness (impermeability) of the coating. However, if the value of the coating is closer to the substrate material, it reflects through-porosity, indicating the open way for exposure solution (NaCl in this study) from the coating surface to interface between coating and substrate. LPCS Cu coating was not fully dense because of existing through-porosity (Fig. 5). The LPCS Ni coating showed similar behavior as the LPCS Cu coating in the open-cell potential measurements. LPCS Ni coating contained also through-porosity (Fig. 6). Electrolytically prepared Ni coating was chosen as a reference sample in this study. In addition, corrosion products from the substrate material (iron oxide) were found by visual examination on the surfaces of LPCS Cu and Ni coatings after exposure. Open-cell potential of LPCS Zn coating was stabilized to the value of −1020 mV. Typically, zinc coating gives cathodic protection to steel substrate, behaving like a sacrificial anode. Because of cathodic protection, denseness (overall dense structure) is not critical for corrosion resistance in the case of zinc coatings.

In addition, denseness of LPCS Cu, Ni, and Zn coatings were tested with salt spray fog test. After exposure, coatings were visually examined. According to visual analysis, corrosion products from substrate material (iron oxide, rust) were detected on the surface of LPCS Cu and Ni coatings, indicating existence of through-porosity. Moreover, only white rust (corrosion product of zinc) was observed on the surface of LPCS Zn coating, indicating sacrificial behavior and at the same time corrosion protection.

According to corrosion tests (open-cell potential measurements and salt spray fog test) LPCS Cu and Ni coatings contained through-porosity. However, steel substrate was protected cathodically by LPCS Zn coating. The addition of ceramic particles has been reported to have an influence on the denseness of the LPCS Al coatings, indicating the possibility of spraying dense coatings with low-pressure cold spray equipment (Ref 5). This will need optimization of powder mixtures and spraying parameters for other coating materials to produce dense coatings with LPCS process.

3.3 Mechanical Properties of LPCS Coatings

3.3.1 Hardness of LPCS Coatings. Hardness of LPCS Cu, Ni, and Zn coatings on both steel and copper substrates is summarized in Table 2. Increased hardness of coatings indicates work hardening due to particle impacts. Somewhat higher hardness values of the LPCS coatings indicated a high level of plastic deformation and strain hardening. Moreover, it should be noticed that Al_2O_3 addition can also have influence on the hardness by increasing the values. The hard phase in the powder mixture was found to have an activation effect of the surface and also a hardening effect, which is seen in the hardness values. Substrate material did not have remarkable influence on the hardness of LPCS Cu, Ni, or Zn coatings.

The hardness of LPCS Cu coating was higher as compared to bulk material than in the cases of LPCS Ni coating. This clearly indicates a higher degree of plastic deformation. The impact may be much stronger in the case of LPCS Cu coating. The hardness of bulk Cu is reported in earlier studies to be $HV_{0.3}$ 90 (Ref 14), which is lower than the value of the LPCS Cu coating. The hardness of high-pressure cold-sprayed (HPCS) Cu and Ni coatings are $HV_{0.1}$ 147 and 238, respectively (Ref 14). The hardness of Ni and Zn bulk materials was $HV_{0.3}$ 111 (stand. dev. 9.0) and 43 (stand. dev. 1.8), respectively. HPCS coatings had higher hardness possibly arising from higher level of plastic deformation. However, it should be noticed that the production method of metallic powder is different and is therefore possibly affecting the hardness values as well. The hardness of LPCS Cu was closer to the value of HPCS Cu than LPCS Ni compared to HPCS Ni coating. This indicates higher level of deformation and more work hardening due to impacts in the case of LPCS Cu particles. In addition, high values of standard deviations (Table 2, stand. dev.) in the hardness measurements of LPCS Ni coatings reflect poor coating quality and very heterogeneous structure.

3.3.2 Bond Strength of LPCS Coatings. The bond strengths of LPCS Cu, Ni, and Zn coatings on both steel and copper substrates were measured with tensile pull tests. Fracture planes were inside the coating, meaning cohesive type fracture. In all the cases, the fracture was found nearer to the interface between coating and substrate but still inside the coating (Table 3).

LPCS Zn coating has significantly high bond strength on both steel and copper substrates, indicating good bonding between coating and substrate, and also between the sprayed particles. Adhesion of LPCS Zn was significantly higher compared to HPCS Zn coating, 13 MPa (Ref 14) on steel substrate arising from the reinforcement effect of Al_2O_3. In this study, all LPCS coatings had the weakest point in the coating. It can be supposed that

Table 2 Hardness ($HV_{0.3}$) of LPCS coatings

Coating	Substrate	Hardness, $HV_{0.3}$	Stand. dev.
Cu	Steel	105	5.3
Cu	Cu	104	3.6
Ni	Steel	119	21.4
Ni	Cu	124	31.7
Zn	Steel	57	0.8
Zn	Cu	57	1.1

Table 3 Bond strength of LPCS coatings

Coating	Substrate	Bond strength, MPa	Stand. dev.
Cu	Steel	20	3.6
Cu	Cu	23	4.1
Ni	Steel	8	3.6
Ni	Cu	9	0.5
Zn	Steel	33	4.7
Zn	Cu	38	0.7

adhesion between coating and substrate was at least the value of the bond (cohesive type) strengths. The bond strength of LPCS Cu coating was also reasonable, 20-23 MPa, and higher than the value of HPCS Cu coating (process gas N_2) on steel substrate (8 MPa) (Ref 14). In the case of LPCS Ni coating, the bond strength was very low, indicating poor bonding between powder particles. Moderate values of bond strengths of LPCS coatings are caused by defects (e.g., pores and imperfect interparticle contacts) and also thin oxide layers between particles (Ref 15), which were also noticed in this study, especially with the LPCS Ni coating. LPCS Ni particles did not undergo as high a plastic deformation as LPCS Cu particles, and thus, the bonds between particles were very moderate due to the possibly stronger oxide layers of powder particles, making even weaker bonding without destroying the oxide layer during impact. On the other hand, ceramic phase has been reported elsewhere to affect adhesion between particles and substrates by increasing it (Ref 5). Lee et al. (Ref 16) have reported that ceramic addition in the powder increased the adhesion of cold-sprayed Al-Al_2O_3 coatings compared to pure Al coating. High adhesion is due to the size of craters between coating and substrate (like activation) (Ref 16). Cohesive type fracture after tensile tests can be explained by poor adhesion between metallic and ceramic particles (Ref 5).

4. Summary

LPCS Cu and Ni coatings were dense according to SEM analysis, whereas through-porosity was observed in the corrosion tests. Some oxidized boundaries and other microscale defects were detected as the weak points in the microstructure, indicating poor bonding and existence of small interparticle porosity. Although the hard phase (Al_2O_3) had a reinforcing effect, it apparently did not hammer the metallic matrix enough to form a dense coating structure (e.g., destroy oxide layers in the powder particle and primary particle boundaries). At least, visually dense and thick coatings can be sprayed with low-pressure cold spraying for applications where corrosion resistance is not crucial (e.g., for electrical and thermal conduction applications). Moreover, LPCS Zn coating was also visually dense and the open-cell potential was electronegative, indicating corrosion resistance behaving like sacrificial anode for the protection of steel substrates.

In this study, mechanical properties were reasonable instead of the bond strength of LPCS Ni coating. High hardness values measured indicated work hardening occurring during spraying. On the other hand, ceramic addition can affect the values. The weak points were at the bonding between particles, indicating cohesive failure type fracture. Therefore, adhesion between particles and substrates was not the most critical point (similar to thermally sprayed coatings).

Optimization of powders, substrates, their combinations, and, moreover, substrate pretreatments and hard phase addition will be investigated in future to produce dense and well-adhered coatings with low-pressure cold spray process.

Acknowledgments

The research was funded by Finnish Funding Agency for Technology and Innovation (TEKES) and a group of Finnish industrial companies.

References

1. C. Borchers, F. Gärtner, T. Stoltenhoff, H. Assadi, and H. Kreye, Microstructural and Macroscopic Properties of Cold Sprayed Copper Coatings, *J. Appl. Phys.*, 2003, **93**(12), p 10064-10070
2. R.G. Maev and V. Leshchynsky, Air Gas Dynamic Spraying of Powder Mixtures: Theory and Application, *J. Therm. Spray Tech.*, 2006, **15**(2), p 198-205
3. A. Kashirin, O. Klyuev, T. Buzdygar, and A. Shkodkin, DYMET Technology Evolution and Application, *Global Coating Solutions: Proceedings of the 2007 International Thermal Spray Conference*, B.R. Marple, M.M. Hyland, Y.C. Lau, C.-J. Li, R.S. Lima, and G. Montavon, Eds., May 14-16, 2007 (Beijing, China), ASM International, p 141-145
4. X.-J. Ning, J.-H. Jang, H.-J. Kim, C.-J. Li, and C. Lee, Cold Spraying of Al-Sn Binary Alloy: Coating Characteristics and Particle Bonding Features. *Surf. Coat. Technol.*, 2008, **202**(9), p 1681-1687
5. E. Irissou, J.-G. Legoux, B. Arsenault, and C. Moreau, Investigation of Al-Al_2O_3 Cold Spray Coating Formation and Properties, *J. Therm. Spray Tech.*, 2007, **16**(5-6), p 661-668
6. X.-J. Ning, J.-H. Jang, and H.-J. Kim, The Effects of Powder Properties on In-Flight Particle Velocity and Deposition Process during Low Pressure Cold Spray Process, *Appl. Surf. Sci.*, 2007, **253**(18), p 7449-7455
7. B.B. Djordjevic and R.G. Maev, SIMAT™ Application for Aerospace Corrosion Protection and Structural Repair, *Building on 100 Years Success: Proceedings of the 2006 International Thermal Spray Conference*, B.R. Marple, M.M. Hyland, Y.C. Lau, R.S. Lima, and J. Voyer, Eds., May 15-18, 2006 (Seattle, Washington, USA), ASM International, 2006
8. A. Shkodkin, A. Kashirin, O. Klyuev, and T. Buzdygar, The Basic Principles of DYMET Technology, *Building on 100 Years Success: Proceedings of the 2006 International Thermal Spray Conference*, B.R. Marple, M.M. Hyland, Y.C. Lau, R.S. Lima, and J. Voyer, Eds., May 15-18, 2006 (Seattle, Washington, USA), ASM International, 2006
9. A. Shkodkin, A. Kashirin, O. Klyuev, and T. Buzdygar, Metal Particle Deposition Stimulation by Surface Abrasive Treatment in Gas Dynamic Spraying, *J. Therm. Spray Tech.*, 2006, **15**(3), p 382-386
10. H. Weinert, E. Maeva, and E. Leshchynsky, Low Pressure Gas Dynamic Spray Forming Near-net Shape Parts, *Building on 100 Years Success: Proceedings of the 2006 International Thermal Spray Conference*, B.R. Marple, M.M. Hyland, Y.C. Lau, R.S. Lima, and J. Voyer, Eds., May 15-18, 2006 (Seattle, Washington, USA), ASM International, 2006
11. R.N. Caron and J.T. Staley, Effects of Composition, Processing, and Structure on Properties of Nonferrous Alloys, Copper and Copper Alloys, *ASM Handbooks Online*, 20, Materials Selection and Design, ASM International, 1997
12. R.N. Caron and J.T. Staley, Effects of Composition, Processing, and Structure on Properties of Nonferrous Alloys, Nickel and Nickel Alloys, *ASM Handbooks Online*, 20, Materials Selection and Design, ASM International, 1997
13. R.N. Caron and J.T. Staley, Effects of Composition, Processing, and Structure on Properties of Nonferrous Alloys, Zinc and Zinc Alloys, *ASM Handbooks Online*, 20, Materials Selection and Design, ASM International, 1997

14. H. Mäkinen (Koivuluoto), J. Lagerbom, and P. Vuoristo, Mechanical Properties and Corrosion Resistance of Cold Sprayed Coatings, *Building on 100 Years Success: Proceedings of the 2006 International Thermal Spray Conference*, B.R. Marple, M.M. Hyland, Y.C. Lau, R.S. Lima, and J. Voyer, Eds., May 15-18, 2006 (Seattle, Washington, USA), ASM International, 2006
15. M. Beneteau, W. Birtch, J. Villafuerte, J. Paille, M. Petrocik, R.G. Maev, E. Strumban, and V. Leshchynsky, Gas Dynamic Spray Composite Coatings for Iron and Steel Castings, *Building on 100 Years Success: Proceedings of the 2006 International Thermal Spray Conference*, B.R. Marple, M.M. Hyland, Y.C. Lau, R.S. Lima, and J. Voyer, Eds., May 15-18, 2006 (Seattle, Washington, USA), ASM International, 2006
16. H.Y. Lee, S.J. Jung, S.Y. Lee, Y.H. You, and K.H. Ko, Correlation between Al_2O_3 Particles and Interface of Al-Al_2O_3 Coatings by Cold Spraying, *Appl. Surf. Sci.*, 2005, **252**, p 2892-2898